PROTEINS
STRUCTURE ■ FUNCTION ■ BIOINFORMATICS

The minimal α-crystallin domain of Mj Hsp16.5 is functional at non-heat-shock conditions

Dong Xi,[1,2] Ping Wei,[2] Changsheng Zhang,[1] and Luhua Lai[1,2]*

[1] BNLMS, State Key Laboratory for Structural Chemistry of Unstable and Stable Species, College of Chemistry and Molecular Engineering, Peking University, Beijing 100871, China

[2] Center for Quantitative Biology, Peking University, Beijing 100871, China

ABSTRACT

The small heat shock protein (sHSP) from *Methanococcus jannaschii* (Mj Hsp16.5) forms a monodisperse 24mer and each of its monomer contains two flexible N- and C-terminals and a rigid α-crystallin domain with an extruding β-strand exchange loop. The minimal α-crystallin domain with a β-sandwich fold is conserved in sHSP family, while the presence of the β-strand exchange loop is divergent. The function of the β-strand exchange loop and the minimal α-crystallin domain of Mj Hsp16.5 need further study. In the present study, we constructed two fragment-deletion mutants of Mj Hsp16.5, one with both the N- and C-terminals deleted (ΔNΔC) and the other with a further deletion of the β-strand exchange loop (ΔNΔLΔC). ΔNΔC existed as a dimer in solution. In contrast, the minimal α-crystallin domain ΔNΔLΔC became polydisperse in solution and exhibited more efficient chaperone-like activities to prevent amorphous aggregation of insulin B chain and fibril formation of the amyloidogenic peptide dansyl-SSTSAA-W than the mutant ΔNΔC and the wild type did. The hydrophobic probe binding experiments indicated that ΔNΔLΔC exposed much more hydrophobic surface than ΔNΔC. Our study also demonstrated that Mj Hsp16.5 used different mechanisms for protecting different substrates. Though Mj Hsp16.5 formed stable complexes with substrates when preventing thermal aggregation, no complexes were detected when preventing aggregation under non-heat-shock conditions.

Proteins 2014; 82:1156–1167.

Key words: Mj Hsp16.5; small heat shock protein; α-crystallin domain; β-strand exchange loop; chaperone-like activity; protein aggregation; mechanism.

INTRODUCTION

Small heat shock proteins (sHSPs) are an ubiquitous class of heat shock proteins that have a monomer size from 12 kDa to 43 kDa and assemble into large oligomers of 9-40 monomers.[1,2] SHSPs show chaperone-like activities to protect other unfolded proteins from aggregation, which is a protection mechanism used by cells from different organisms. As sHSPs are associated with many protein misfolding diseases such as cataracts, Alzheimer's disease and Parkinson's disease, investigations on the relationship between the structure and the function of sHSPs will provide useful information to understand the mechanisms of these diseases.[3–5]

Mj Hsp16.5 is a sHSP from *Methanococcus jannaschii*. Chaperone-like activities of Mj Hsp16.5 have been reported for many substrates *in vitro*.[6–9] Mj Hsp16.5 shows efficient chaperone-like activities to prevent the thermal aggregation of single-chain monellin (SCM) and *Escherichia coli* cell extract at 80°C, and a tight complex is formed between Mj Hsp16.5 and SCM.[6,9] However, Mj Hsp16.5 is an inefficient chaperone in preventing the dithiothreitol (DTT)-induced aggregation of the insulin

Additional Supporting Information may be found in the online version of this article.

Abbreviations: CD, circular dichroism; CS, citrate synthase; DTT, dithiothreitol; FRET, fluorescence resonance energy transfer; PBS, phosphate buffer saline; sHSP, small heat shock protein; WT, wild-type Mj Hsp16.5; ΔNΔC, Mj Hsp16.5 mutant protein lacking the N-terminal and the C-terminal; ΔNΔLΔC, Mj Hsp16.5 mutant protein lacking the N-terminal, the C-terminal, and the β-strand exchange loop.

Grant sponsor: Ministry of Science and Technology of China and National Natural Science Foundation of China.
*Correspondence to: Luhua Lai, College of Chemistry and Molecular Engineering, Peking University, Beijing 100871, China. E-mail: lhlai@pku.edu.cn
Received 15 July 2013; Revised 28 October 2013; Accepted 9 November 2013
Published online 16 November 2013 in Wiley Online Library (wileyonlinelibrary.com). DOI: 10.1002/prot.24480

B chain at 37°C.[7] The underlying mechanism of the substrate-dependent chaperone-like activities of Mj Hsp16.5 needs to be further explored.

The crystal structure reveals that Mj Hsp16.5 is a homomeric 24mer with a hollow spherical shape and octahedral symmetries. The sHSP family is highly conserved and has similar monomer protein structure. The monomer of Mj Hsp16.5 can be segmented as three domains: the highly disordered N-terminal domain (residues 1–33), the C-terminal domain (residues 136–147), and the entire α-crystallin domain (residues 34–135), which is composed of a rigid β-sandwich (the minimal α-crystallin domain) and an extruding β-strand exchange loop (residues 87–98).[1] As the first reported crystal structure for sHSP, the structure of Mj Hsp16.5 has been widely used in comparing with or building structure models for other sHSP.[4,10,11] The minimal α-crystallin domain is the most conserved region in the sHSP family, while the sequence and structure conservation of the N- and C-terminals are low and the presence of the extruding β-strand exchange loop in the α-crystallin domain are divergent.[1,10,12,13]

How these non-conserved fragments and the conserved minimal α-crystallin domain of Mj Hsp16.5 contribute to its oligomer assembly and chaperone-like function remain to be understood. The N-terminal domain was reported to be necessary for the chaperone-like activity of many sHSPs.[6,14,15] Since the minimal α-crystallin domain is the most conserved part in the sHSP family, it is interesting to know whether the minimal α-crystallin domain alone is sufficient for the chaperone-like activities. The β-strand exchange loop is another important and interesting fragment of Mj Hsp16.5. The 24mer structure of Mj Hsp16.5 is assembled from dimer building blocks and each of the dimer is formed by two monomers with a domain swapping structure using this β-strand exchange loop.[1] Sequence alignment indicates that the long β-strand exchange loop exists in Mj Hsp16.5 and wheat Hsp16.9, while the loop is very short in mammalian sHSPs, such as mammalian (human, bovine, and murine) αA-crystallin, αB-crystallin, Hsp27.[1,4,10,16,17] The importance of this loop is also supported by the fact that mutations in this loop of mammalian sHSPs are correlated with certain congenital disease such as Charcot-Marie-Tooth disease.[18,19] Understanding the function of this loop region in Mj Hsp16.5 will be helpful to uncover the evolutional difference from Mj Hsp16.5 to mammalian sHSPs, and to understand the mechanisms of the related diseases.

In the present study, we investigated the function of the non-conserved fragments and the conserved minimal α-crystallin domain of Mj Hsp16.5. Two fragment-deletion mutant proteins of Mj Hsp16.5, ΔNΔC (mutant deleting the N-terminal and the C-terminal), and ΔNΔLΔC (mutant deleting the N-terminal, the C-terminal and the β-strand exchange loop) were constructed. Their oligomer state, chaperone-like activities, hydrophobic surface, and the properties of complex formation with different substrates were studied. Mj Hsp16.5 was found to use different mechanisms of chaperone-like activities for different substrates.

MATERIALS AND METHODS

Materials

Rosetta (DE3), pGEX 4T-1 plasmid, T7 promoter, and terminator primers were from Novagen. The pET21a plasmid containing the Mj Hsp16.5 gene was a generous gift from Professor Sung-Hou Kim at the University of California, Berkeley. Primers for mutation were synthesized by Boya company. Citrate synthase (CS) from porcine heart, insulin from bovine pancreas, 4,4′-dianilino-1,1′-binaphthyl-5,5′-disulfonic acid dipotassium salt (bis-ANS), bovine serum albumin, ovalbumin from chicken egg white, trypsin inhibitor from soybean, cytochrome C from horse heart, and mineral oil were from Sigma. Water was of Millipore quality. All other chemicals were of analytical grade or higher.

Mutant plasmid construction

The fragment-deleted mutants were constructed as follows: Single-fragment-deleted mutants: ΔN (the N-terminal 33 amino acid residues were omitted by designing a 5′ primer which began matching with the wild-type (WT) template at residue 34) and ΔC (the C-terminal 12 amino acid residues were omitted by changing the WT template at residue 136 to a stop codon), and ΔL [amino acid residues 87–98 MITESERIIYSE were replaced by SGG using polymerase chain reaction (PCR) long primer mutagenesis]. Double-fragment-deleted mutants were constructed based on the single-fragment-deleted mutants by PCR amplification as follows: ΔNΔC (template: ΔC, 5′ primer was the same as the ΔN 5′ primer); and ΔLΔC (template: ΔL, 3′ primer: 136 stop codon primer). The triple-fragment-deleted mutant ΔNΔLΔC was constructed by PCR amplification, using ΔLΔC as template and the ΔN 5′ primer as 5′ primer. The primers not mentioned previously were T7 promoter or terminator primers. The mutants ΔN, ΔNΔC, and ΔNΔLΔC were constructed using plasmid pGEX4T-1. Two residues, Gly and Ala, were added to the N terminal of these mutant proteins, due to the Glutathione-S-transferase (GST) fusion protein expression system.

Mutant protein expression and purification

All plasmids were transformed to Rosetta (DE3) for expression. The fragment-deleted mutant proteins ΔNΔC and ΔNΔLΔC were purified using the GST fusion method. Rosetta (DE3) were grown to the exponential phase at 37°C, then expression of fusion protein was

induced by adding 0.5 m*M* isopropyl-1-thio-β-D-galactopyranoside at 25°C for 5 h. The cell pellet was collected by centrifugation (4°C, 8000 rpm with rotor JLA-8.1 from Beckman Coulter, 10 min), and stored at −80°C. For protein purification, the pellet was resuspended in cell lysis buffer [30 mL phosphate buffered saline (PBS) buffer with 5 m*M* ethylenediaminetetraacetic acid, 0.3 m*M* phenylmethylsulfonyl fluoride, and 1 m*M* DTT for 1 L of culture], then sonicated using a probe-tip sonicator for 200 cycles (each cycle contained 3 s of sonication and 5 s rest). The lysate was centrifuged (4°C, 18,000 rpm with rotor R20A2 from Hitachi, 20 min). The supernatant, precipitate and cell lysate were analyzed by sodium dodecyl sulfate polyacrylamide gel electrophoresis (SDS-PAGE) to verify that the fusion protein was mainly in the supernatant. A series of affinity chromatography columns were applied to purify the mutant proteins. The supernatant of the cell lysate was loaded onto a pre-equilibrated glutathione column (Hitrap GSTrap FF, GE) in buffer A (50 m*M* PBS, pH 7.3, 150 m*M* NaCl). The GST-fusion protein was cleaved on column by the addition of 10 units of thrombin (GE) for each milligram of GST-fusion protein in buffer A at 25°C for 10 h to remove the GST tag from the aimed proteins. Then, the elute containing the products in the unbounded fraction after enzyme digestion were loaded onto a pre-equilibrated glutathione column (Hitrap GSTrap FF,GE) in buffer A again to remove GST and undigested fusion proteins, which was eluted a little in the previous step. The elute of the unbound fraction was then loaded onto a benzamidine sepharose column (HiTrap Benzamidine FF,GE) to remove thrombin. The final product in the unbound fraction was concentrated by ultracentrifugation (4°C, 4500 rpm with rotor SX4250 from Beckman Coulter) with Amicon Ultra-15 centrifugal 3K filter devices from Millipore. The fractions from each intermediate procedure were analyzed by SDS-PAGE. Protein bands were stained with Coomassie brilliant blue.

Mass spectrum identification of mutant proteins

An Autoflex III mass spectrometry with a matrix-assisted laser desorption/ionization device (Bruker Daltonics GmbH, Germany) was used to identify the molecular weight and purity of the purified mutant proteins. Proteins were predesalted to 20 m*M* PBS (pH 7.3) buffer before measurement. MAIDI-TOF mass spectra showed the purity of both proteins, and the molecular weight of ΔNΔC was 11,497 Da, while that of ΔNΔLΔC was 10,242 Da.

Circular dichroism

Circular dichroism (CD) spectra were recorded for the WT Mj Hsp16.5 and the mutants ΔNΔC, ΔNΔLΔC on a MOS 450 AF/CD (Biologic, France) at different temperatures, with 1 mm path length cylinder quartz cuvettes for far ultraviolet (UV) region (190–260 nm). The concentrations of the three proteins were all 0.2 mg mL^{-1}. Proteins were predesalted to 40 m*M* PBS buffer (pH 7.3) before measurements. Each CD spectra represents the average of three scans.

Thermal denaturation curves of the mutant proteins ΔNΔC and ΔNΔLΔC were also recorded on the MOS 450 AF/CD using the Peltier accessory with 1 cm quartz cuvettes. The CD signal at 216 nm was recorded. The concentration of the two proteins was 0.1 mg mL^{-1} in 40 m*M* PBS buffer (pH 7.3), and heating was performed at the speed of 1°C min^{-1} from 25°C to 95°C.

Buffer condition

All the experiments of the chaperone-like activities assay, bis-ANS binding experiments and the gel filtration analyses were carried out with the same physiological buffer A (50 m*M* PBS, pH 7.3, 150 m*M* NaCl).

Protein concentration measurement

The concentrations of Mj Hsp16.5 and the two mutant proteins ΔNΔC, ΔNΔLΔC were determined by absorbance at 280 nm using a UV/visible (Vis) spectrometer Ultrospec 1100 pro (Amersham Biosciences) with extinction coefficients of 0.502 $mg^{-1}cm^2$ (WT), 0.719 $mg^{-1}cm^2$ (ΔNΔC) and 0.680 $mg^{-1}cm^2$ (ΔNΔLΔC), respectively. All the extinction coefficients were theoretic value calculated from the amino acid sequences using the Vector NTI software from Invitrogen,[20] since we used these determined concentration to compare the chaperone-like activities of the mutant proteins with the WT. Bradford method was also used to validate the concentration determined by the theoretic extinction coefficients. The errors of the two methods for the three proteins were below 20%.

Oligomeric state determination by size exclusion chromatography

Different concentrations of purified mutant proteins were loaded onto an analytical size exclusion chromatography column (Superdex-75 10/300 GL, GE) pre-equilibrated with buffer A. The protein molecular markers ovalbumin from chicken egg white (43.1 kDa), trypsin inhibitor from soybean (20.1 kDa), and cytochrome C from horse heart (12.3 kDa) were used as molecular weight standards.

Chaperone-like activity assay for the insulin substrate

The aggregation of reduced insulin at 37°C triggered by DTT (2 m*M*) were monitored by light scattering at 360 nm using a multiwell UV spectrometer SpectraMax 190 (Molecular Device) with a 96-well plate. Insulin was

first dissolved as high concentration in 20 m*M* Gly-HCl buffer (pH 3.0). The concentration of insulin was determined by absorbance at 280 nm using a UV/Vis spectrometer Ultrospec 1100 pro (Amersham Biosciences) with the extinction coefficients of 1.00 mg^{-1} cm^2. Different concentrations of the mutant proteins and the WT were mixed with the substrate insulin (50 μ*M*) to show the concentration dependence. These experiments were repeated three times, and the results shown are representative of one of these experiments with all the samples prepared and measured at the same time and conditions. The quantitative difference between different repeats is less than 20%.

Chaperone-like activity assay for the amyloidogenic peptide dansyl-SSTSAA-W substrate

The modified amyloidogenic peptide SSTSAA with a dansyl group at the N-terminal and a tryptophan residue at the C-terminal was synthesized by standard Fmoc synthesis.[21] The lyophilized peptide was dissolved in water by sonication for 5 s and filtered by the filter membrane (0.22 μm). The concentration of the peptide was determined by the absorbance at 280 nm using a UV/Vis spectrometer Ultrospec 1100 pro (Amersham Biosciences) with the theoretic extinction coefficients of 10.0 mg^{-1} cm^2. The WT and the mutant ΔNΔC, ΔNΔLΔC with the same molar concentration of the monomer (15 μ*M*) were separately incubated with the amyloidogenic peptide (150 μ*M*) solution. Amyloid fibril formation process was monitored by the change in the fluorescence emission spectrum of the reaction mixture before and after 24 h incubation in Buffer A at room temperature. The emission spectrum from 340 nm to 550 nm with the excitation wavelength of 295 nm was scanned by the FluoroLog 3 Spectrofluorometer (HORIBA Jobin Yvon, Longjumeau, France). These experiments were repeated three times and the results shown are representative of one of these experiments with all the samples prepared and measured at the same time and conditions. The order of the chaperone-like activities of the three proteins is consistent among all repeats.

Chaperone-like activity assay for the CS substrate

The thermal aggregation of CS at 50°C was monitored by light scattering at 360 nm using a Lambda 45 UV/Vis spectrometer (Perkin Elmer) with the temperature controlled by a digital temperature controller (PolyScience). In all aggregation assay experiments, 10 μL of mineral oil was added to prevent evaporation. The concentration of CS was determined by absorbance at 280 nm using a UV/Vis spectrometer Ultrospec 1100 pro (Amersham Biosciences) with the extinction coefficients of 1.78 mg^{-1} cm^2. The concentrations of each reaction constituents were: CS (0.67 μ*M* of the monomer) and the chaperone (64 μ*M* of the monomer). The preheating of WT and mutant proteins was performed by incubating them in a water bath at 85°C for an hour, and then cooling in air to room temperature. These experiments were repeated three times and the results shown are representative of one of these experiments with all the samples prepared and measured at the same time and conditions. The quantitative difference between different repeats is less than 20%.

Bis-ANS binding experiment

The hydrophobic probe bis-ANS at a final concentration of 2 μ*M* was separately mixed with WT Mj Hsp16.5 and the mutants ΔNΔC, ΔNΔLΔC at the same molar concentration of the monomer (2 μ*M*) in physiological buffer A. The mixture samples were preincubated separately at room temperature, 37°C and 50°C (using thermal cycler from Eppendorf) for an hour and cooling to room temperature for measurements. Binding spectra were acquired by a FluoroLog 3 Spectrofluorometer (HORIBA Jobin Yvon) with a 1-cm path length cuvette. Samples were excited at 385 nm, and the emission was recorded from 400 nm to 600 nm. The excitation and emission slit width were set to 5 nm. Each bis-ANS spectrum represents the average of three scans. The concentration of bis-ANS was determined by absorbance at 385 nm with an extinction coefficient ε_{385} = 16,790 cm^{-1} M^{-1},[22] using a NanoDrop 2000 spectrophotometer from Thermo Scientific.

Gel filtration analysis of the chaperon–substrate complex

The chaperone was mixed with different substrates separately and aggregation assays for chaperone-like activities were carried out to guarantee the complete suppression of the aggregation. The reaction mixture for all the aggregation assays were centrifuged (12,000 rpm, 5 min), and filtered by the filter membrane (0.22 μm), then loaded onto the analytical size exclusion chromatography column (Superose-6 10/300, GE) pre-equilibrated with buffer A.

Structure model generation

The structure model of the monomeric ΔNΔLΔC was generated by mutation from the WT Mj Hsp16.5 with PyMol[23] and energy minimization with GROMAC.[24]

RESULTS

The secondary structures were retained in the mutant proteins

We constructed three fragment-deletion mutant proteins of Mj Hsp16.5 [Fig. 1(A)]. The ΔNΔC and ΔNΔLΔC mutants were expressed and purified in the *E. coli* as GST-fusion proteins, while the ΔN mutant cannot

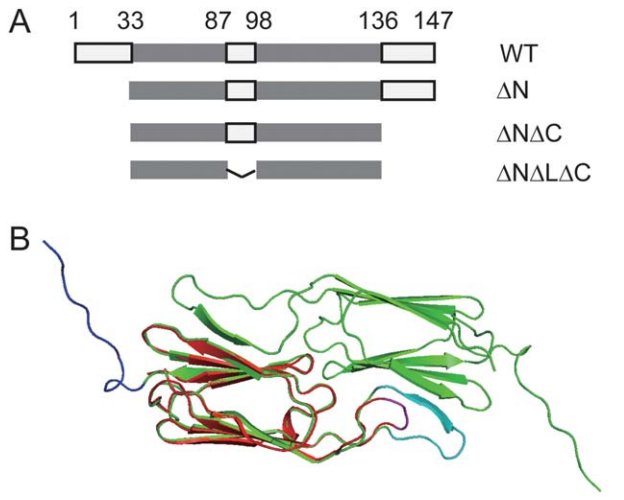

Figure 1

Domain structure of the mutants. (**A**) Domain structure of Mj Hsp16.5 mutants constructed in this study: ΔN (the N-terminal 33 amino acid residues were omitted, ΔNΔC (the N-terminal 33 amino acid residues and the C-terminal 12 amino acid residues were omitted), and ΔNΔLΔC (the N-terminal 33 amino acid residues and the C-terminal 12 amino acid residues were omitted and the amino acid residues 87–98 MITESERIIYSE in the β-strand exchange loop were replaced by SGG). (**B**) Superposition of the monomeric ΔNΔLΔC (red) on a dimer of wild-type Mj Hsp16.5 (green). The amino acid residues 87–98 MITESERIIYSE (cyan) in the wild type were replaced by SGG (magenta) in ΔNΔLΔC. The C-terminal of the wild type was shown in blue while the N-terminal was not seen from the crystal structure. Superposition was made with PyMOL.[23]

be purified due to its gel characteristic, as reported by Kim *et al.*[6] The mutant proteins ΔNΔC and ΔNΔLΔC were successfully purified using a series of affinity chromatography columns.

Far UV CD spectra showed that the mutant proteins retained a β-sheet core structure, indicated by the negative peak at 215 nm [Fig. 2(A)]. This negative peak showed a blue-shift compared with the WT Mj Hsp16.5, indicating the removal of other non-β structures. Compared to the WT protein, the mutant proteins contain an increased amount of random coil structures as indicated by a weak peak at 195 nm. The far UV CD spectra of the mutant ΔNΔC showed no difference at higher temperatures [Fig. 2(B)], while the CD spectra of the mutant ΔNΔLΔC changed at 85°C and 95°C [Fig. 2(C)]. Thermal denaturation experiment demonstrated that both mutants were heat stable, and the mutant ΔNΔC was more stable than the mutant ΔNΔLΔC, which began to denature above 85°C [Fig. 2(D)].

The two mutant proteins exhibited different types of quaternary structure

The crystallographic study of Mj Hsp16.5 indicated that the three non-conserved fragments play important roles in its oligomerization.[1] After deleting the fragments, the mutant proteins displayed different oligomeric states in gel filtration experiments (Fig. 3). The mutant ΔNΔC eluted as a single peak, independent of sample concentration, which was corresponding to an apparent molecular weight of 28 kDa, and could be considered as a dimer. In contrast, the mutant ΔNΔLΔC existed as a polydisperse quaternary structure, with a combination of oligomers of different size as indicated by shoulder elution peaks. The oligomeric state of ΔNΔLΔC showed clear concentration dependence. The main peak shifted to the smaller oligomer when the concentration was low and to the larger oligomer when the concentration was high.

The mutant protein ΔNΔLΔC exhibited even better chaperone-like activity to the insulin B chain substrate

The B chain of insulin aggregates after being induced by the addition of DTT, and is a commonly used substrate to measure chaperone-like activity *in vitro*.[7,12,14,25] The WT Mj Hsp16.5 is an inefficient chaperone for this substrate at 37°C. A molar ratio of 8:1 of Mj Hsp16.5 monomer to insulin was needed to completely inhibit the aggregation [Fig. 4(A)]. The mutant protein ΔNΔC showed less efficient chaperone-like activity than the WT, and a molar ratio of 8:1 was not enough to completely inhibit the aggregation [Fig. 4(B)]. Surprisingly, ΔNΔLΔC showed better chaperone-like activity to the insulin substrate than the WT at 37°C. A molar ratio of 2:1 of the ΔNΔLΔC monomer to insulin was enough to completely inhibit the aggregation of insulin B chain induced by DTT [Fig. 4(C)].

The mutant protein ΔNΔLΔC exhibited even better chaperone-like activity to inhibit the aggregation of an amyloidogenic peptide

In a previous study, we showed that Mj Hsp16.5 can inhibit the amyloid fibril formation process of a peptide from RNase with a FRET pair attached: dansyl-SSTSAA-W.[8] The introduction of the FRET pair provides a useful tool to monitor the time course of amyloid fibril formation.[21,26] We used this peptide as another substrate to measure the *in vitro* chaperone-like activity of sHSPs at room temperature. The WT and the mutant ΔNΔC, ΔNΔLΔC were separately mixed with the peptide in the same molar concentration of the monomer. The fibrils formed in the WT and ΔNΔC samples after 24 h incubation at room temperature, as indicated by the FRET signal of the tryptophan and the dansyl group from two mating β-sheets in the process of fibril formation of the peptide, while no fibrils formed in the ΔNΔLΔC sample (Fig. 5). This result demonstrated that the chaperone-like activity of the mutant ΔNΔLΔC was more effective than the mutant ΔNΔC and the WT protein in inhibiting the formation of amyloid fibrils at room temperature.

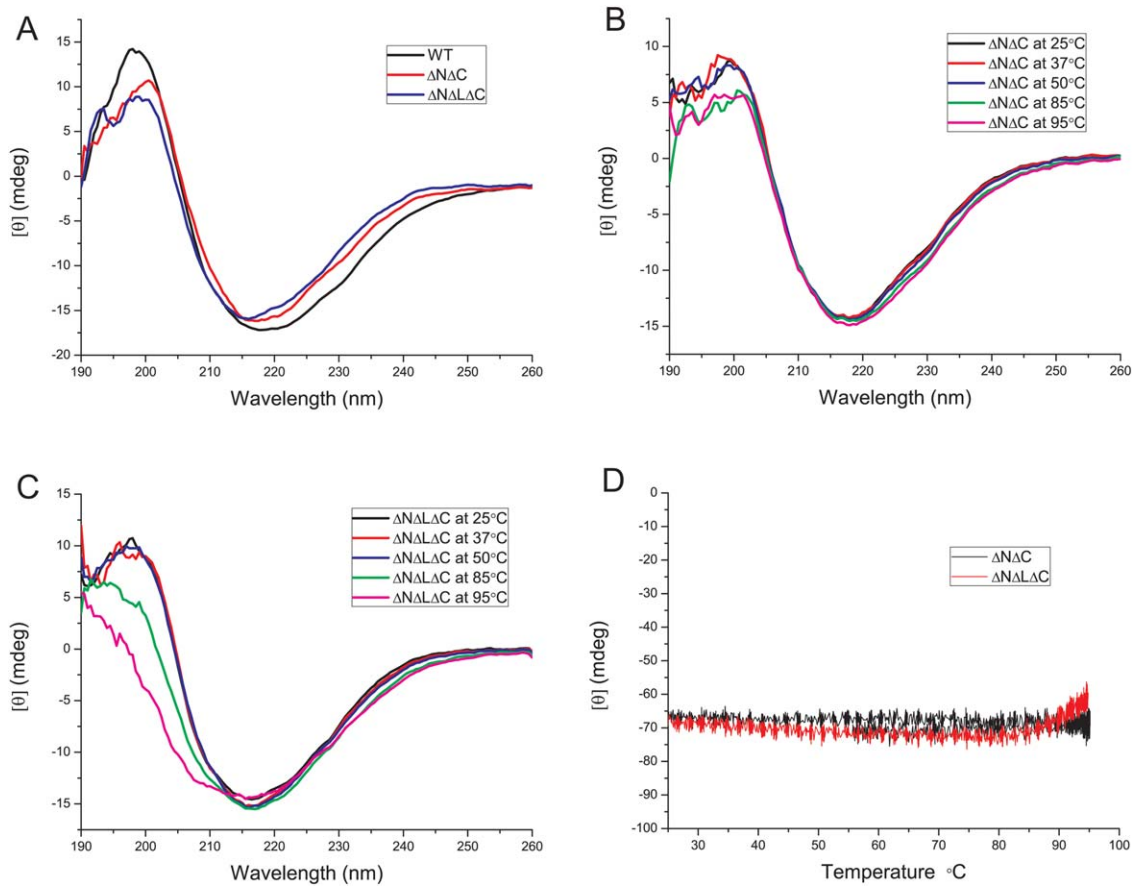

Figure 2

Far UV CD spectra and thermal denaturation of the mutants. (**A**) Far UV CD spectra of the two mutants ΔNΔC and ΔNΔLΔC along with the wild-type Mj Hsp16.5. The concentration of the three proteins was all 0.2 mg mL^{-1}. (**B**) Temperature dependence of the CD spectra for the mutant ΔNΔC with the concentration of 0.2 mg mL^{-1}. (**C**) Temperature dependence of the CD spectra for the mutant ΔNΔLΔC with the concentration of 0.2 mg mL^{-1}. (**D**) Thermal denaturation of the mutants ΔNΔC and ΔNΔLΔC detected by the CD signal at 216 nm with the concentration of 0.1 mg mL^{-1}. [Color figure can be viewed in the online issue, which is available at wileyonlinelibrary.com.]

The mutant proteins failed to suppress the thermal aggregation of CS

We further investigated the *in vitro* chaperone-like activity of the two mutant proteins using CS as a substrate, which aggregates at above 42°C. The WT Mj Hsp16.5 is reported to exhibit increased chaperone-like activity in suppressing the thermal aggregation of CS after preheating.[2] We found that the two mutant proteins showed no chaperone-like activity for the CS substrate at 50°C, both with and without preheating [Fig. 6(B,C)], while the WT exhibited chaperone like-activity to suppress the thermal aggregation at the same molar concentration of the monomer as the two mutants [Fig. 6(A)].

The mutant protein ΔNΔLΔC exposed more hydrophobic surface than ΔNΔC

The two mutant proteins ΔNΔLΔC and ΔNΔC, differing only in the β-strand exchange loop, exhibited dramatically different chaperone-like activities to prevent amorphous aggregation of insulin B chain and fibril formation of the amyloidogenic peptide dansyl-SSTSAA-W at non-heat-shock conditions. To further investigate the difference of their hydrophobic surface exposure, bis-ANS, a fluorescent dye that can access the hydrophobic surface of proteins was used. With the excitation wavelength of 385 nm, the proteins Mj Hsp16.5, ΔNΔLΔC, ΔNΔC alone generated no meaningful fluorescence signal, and bis-ANS alone showed weak fluorescence at 524 nm. However, after mixed with the proteins, bis-ANS showed high fluorescence signal with the peak blue shifted to around 500 nm by binding to the hydrophobic surface of the proteins. In our experiments, bis-ANS were all in excess, and the relative fluorescence intensity indicated the extent of the hydrophobic surface exposure of the proteins. At the same molar concentration of monomer, the mutant ΔNΔLΔC exposed much more hydrophobic surface than the mutant ΔNΔC at various temperatures for incubation, indicated by the higher

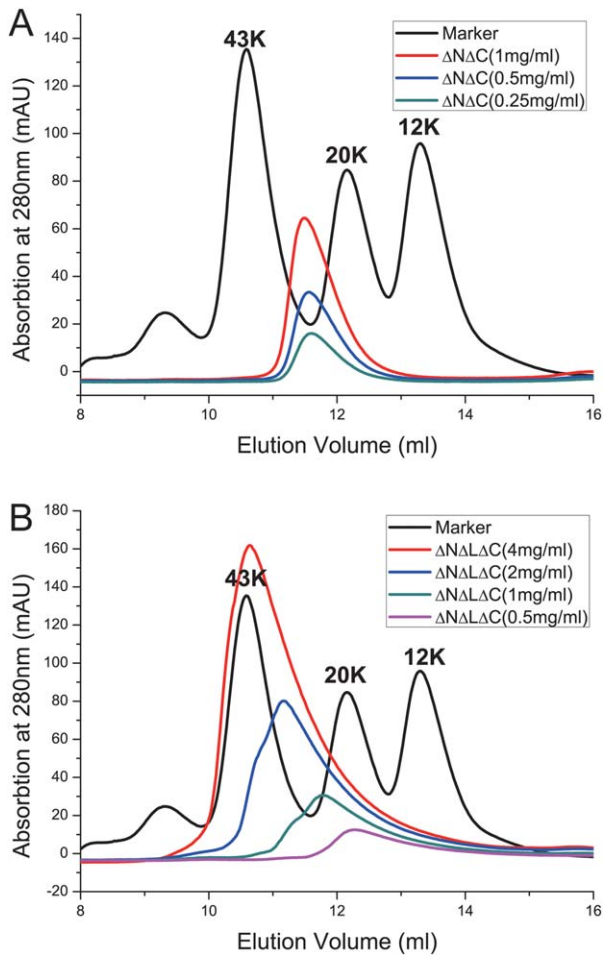

Figure 3

Size exclusion chromatography elution curves of the two mutants ΔNΔC and ΔNΔLΔC. (**A**) Elution curves of ΔNΔC at concentrations from 0.25 mg mL^{-1} to 1 mg mL^{-1}. (**B**) Elution curves of ΔNΔLΔC at concentrations from 0.5 mg mL^{-1} to 4 mg mL^{-1}. Only the elution volume from 8 mL to 16 mL is shown for clarity; the entire column volume was 24 mL, but no peaks occurred below 8 mL and above 16 mL. [Color figure can be viewed in the online issue, which is available at wileyonlinelibrary.com.]

fluorescence intensity (Fig. 7 and Supporting Information Fig. S1). At the same molar concentration of monomer, the minimal α-crystallin domain ΔNΔLΔC exposed comparable hydrophobic surface as the WT Mj Hsp16.5 (Fig. 7 and Supporting Information Fig. S1).

Gel filtration analysis of complex formation between the chaperone and different substrates

Since the WT and the mutants exhibited different behavior on different substrates, gel filtration was used to further investigate the possible complex formation between Mj Hsp16.5 and substrates. We compared the elution curves of the reaction mixture before and after being triggered by the factors that induce the unfolding process of the substrates. The mixtures of Mj Hsp16.5 and the substrates were all at molar ratios at which Mj Hsp16.5 completely suppressed the substrate aggregation.

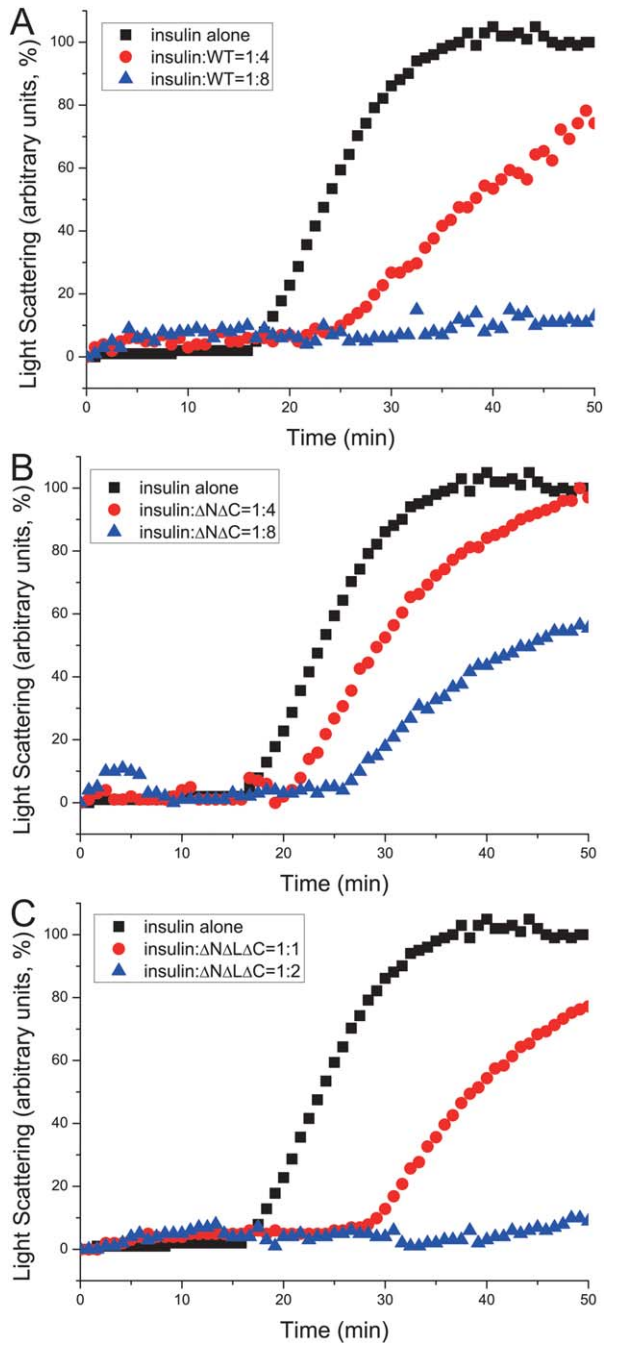

Figure 4

Chaperone-like activities of mutant and wild-type proteins to suppress aggregation of insulin B chain. (**A–C**) Kinetics of normalized light scattering of aggregation of insulin (50 μ*M*) triggered by DTT (2 mM) at 37°C in the presence of wild type with monomer molar concentration dependence of 200 μ*M* and 400 μ*M* (A), ΔNΔC with monomer molar concentration dependence of 200 μ*M* and 400 μ*M* (B), and ΔNΔLΔC with monomer molar concentration dependence of 50 μ*M* and 100 μ*M* (C). [Color figure can be viewed in the online issue, which is available at wileyonlinelibrary.com.]

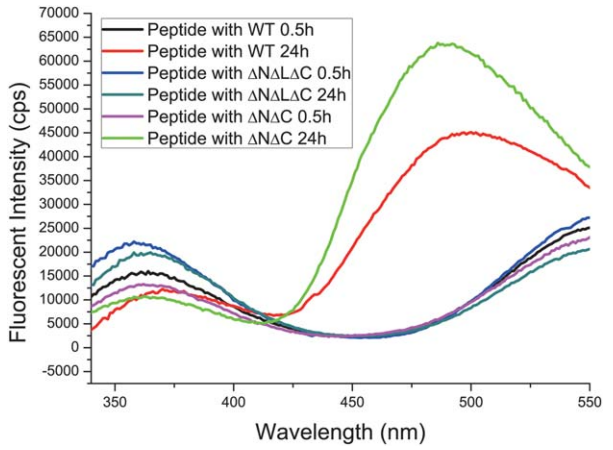

Figure 5

Chaperone-like activities of mutant and wild-type proteins to suppress the fibril formation of the modified peptide dansyl-SSTSAA-W. The fluorescence emission spectroscopy of the peptide (150 μ*M*) before and after incubation with the same monomer molar concentration (15 μ*M*) of the wild type and the mutants ΔNΔC, ΔNΔLΔC for 24 h at room temperature. [Color figure can be viewed in the online issue, which is available at wileyonlinelibrary.com.]

When the insulin B chain or the amyloidogenic peptide dansyl-SSTSAA-W substrates were used, no peak for a larger chaperone–substrate complex was observed for the WT Mj Hsp16.5 [Fig. 8(A,B)] and ΔNΔLΔC, ΔNΔC mutants (data not shown), indicating no tight complexes were formed. For the CS substrate, a peak corresponding to the chaperone–substrate complex appeared in the void volume and the peak for CS disappeared after being triggered [Fig. 8(C)].

DISCUSSION

The minimal α-crystallin domain alone is sufficient to suppress protein or peptide aggregation under non-heat-shock conditions

The immunoglobulin-like α-crystallin domain is the most conserved elements in sHSPs.[1,12,13,27] The minimal α-crystallin domain of *Saccharomyces cerevisiae* Hsp26 was found to be able to exist as a stably folded monomer[28]; however, chaperone-like activity was not reported. Whether the chaperone-like activity of sHSPs depends on the most conserved α-crystallin domain is still an open question. Many studies show that the N-terminal domain of sHSPs is essential for the chaperone-like activities.[6,14,15,29–32] The N-35 deletion mutant of *Mycobacterium tuberculosis* Hsp16.3 fails to protect against the aggregation of insulin B chain.[14] The truncated α-crystallin domain of human αB-crystallin (αB57-157) is functional to inhibit the aggregation of alcohol dehydrogenase (ADH) at 37°C, though its chaperone-like activity is less efficient than the WT.[33] The truncated form of human αB-crystallin (αB68–162) containing C-terminal extension also exhibits chaperone like activity for ADH and moderate chaperone-like

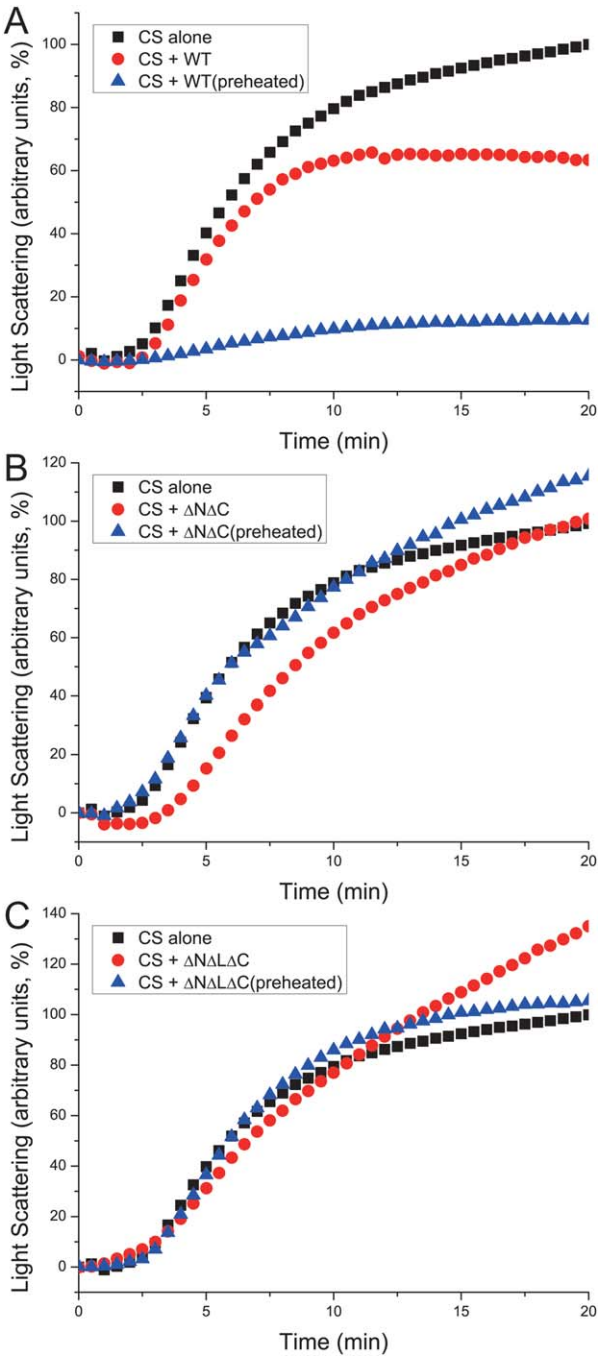

Figure 6

Chaperone-like activities of the mutant and wild-type proteins to suppress thermal aggregation of CS. (**A**–**C**) Kinetics of normalized light scattering of thermal aggregation of CS (0.67 μ*M* of the monomer) at 50°C in the presence of the chaperone: wild type (A), ΔNΔC (B), and ΔNΔLΔC (C). All these chaperone, with and without preheating were at the same concentration (64 μ*M* of the monomer). [Color figure can be viewed in the online issue, which is available at wileyonlinelibrary.com.]

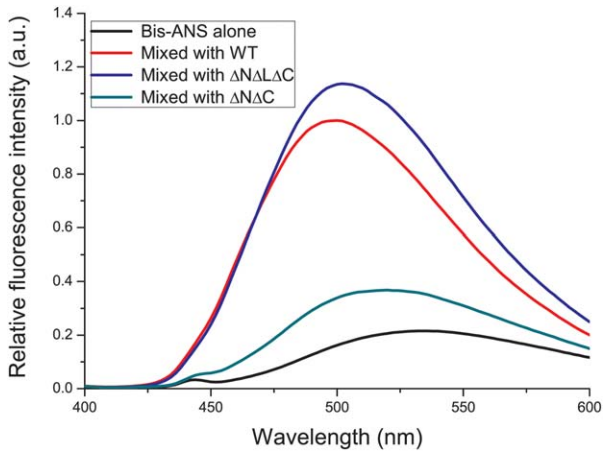

Figure 7

Bis-ANS binding experiments to detect the hydrophobic surface exposure. Bis-ANS at a final concentration of 2 μ*M* was separately mixed with wild type Mj Hsp16.5 and the mutants ΔNΔC, ΔNΔLΔC at the same final molar concentration of the monomer (2 μ*M*) in physiological buffer A. The mixture samples were preincubated at 37°C for an hour before measurements. Fluorescence spectra were recorded at room temperature with excitation at 385 nm and emission scan from 400 nm to 600 nm. The three proteins alone generated no meaningful fluorescence signal. The relative fluorescence intensity of all samples was normalized by setting the peak value of the wild-type sample as 1. [Color figure can be viewed in the online issue, which is available at wileyonlinelibrary.com.]

activity for lactalbumin.[16] Our results showed that the mutant ΔNΔLΔC of Mj Hsp16.5, with all the non-conserved fragments deleted and retaining only the conserved β-sandwich, exhibited even better chaperone-like activity for insulin B chain. A monomer molar ratio to insulin of 2:1 was enough to completely suppress the aggregation, which was four times more efficient than the WT Mj Hsp16.5. We also used the modified amyloidogenic peptide dansyl-SSTSAA-W as another substrate to investigate the chaperone-like activity of the mutant ΔNΔLΔC compared with the WT at room temperature. The mutant ΔNΔLΔC also exhibited better activity than the WT. These results suggest that neither the oligomeric structure of the 24mer, nor the non-conserved fragments are necessary for the chaperone-like activities of Mj Hsp16.5 for these two substrates. The conserved minimal α-crystallin domain alone is sufficient to exhibit chaperone-like activity to suppress aggregation of the two substrates under our experiment conditions.

The β-strand exchange loop covers the hydrophobic surface for binding substrates

Bis-ANS experiment demonstrated that the minimal α-crystallin domain ΔNΔLΔC exposed more hydrophobic surface than the entire α-crystallin domain ΔNΔC and exhibited more efficient chaperone-like activities to prevent amorphous aggregation of insulin B chain and

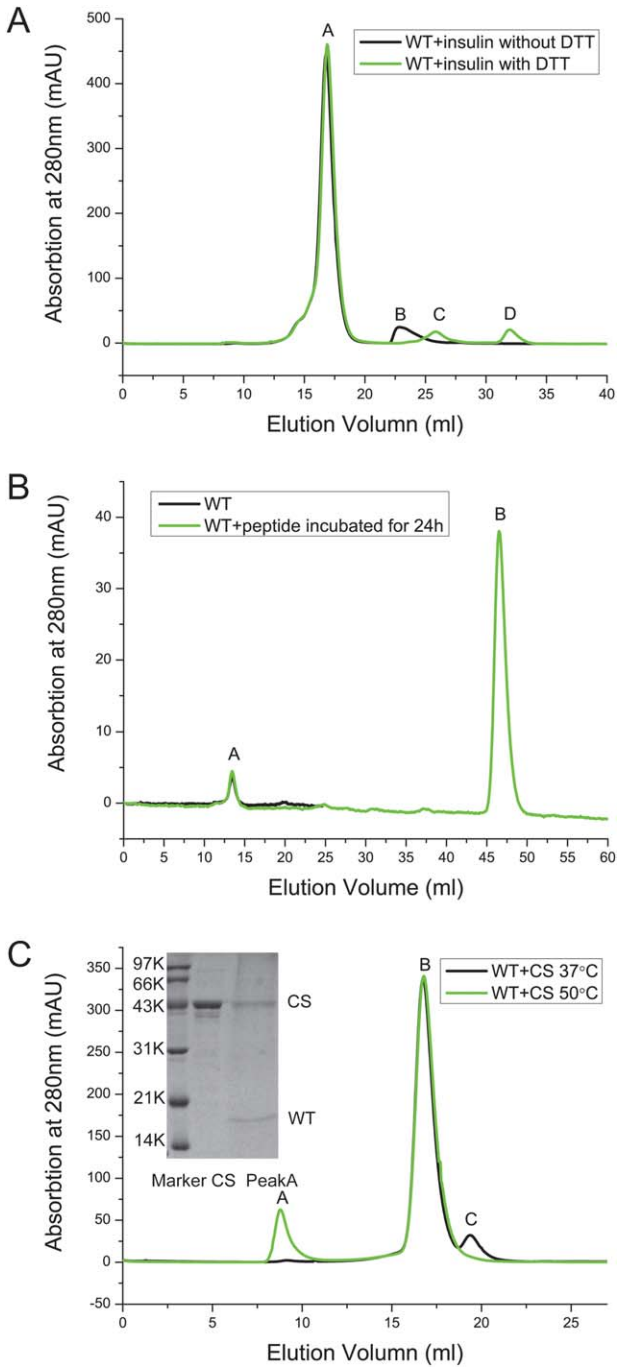

Figure 8

Analysis of the complex formation between the chaperone and different substrates by gel filtration. (**A**–**C**) Size exclusion chromatography elution curves of the mixture of the chaperone and substrates with and without being triggered aggregation. (A) Mixture of the wild type and insulin (peak A represents the wild type Mj Hsp16.5; peak B represents the intact insulin; peak C represents the insulin chain; and peak D represents DTT). (B) Mixture of the wild type and the peptide dansyl-SSTSAA-W (peak A represents the wild type Mj Hsp16.5; peak B represents the peptide). (C) Mixture of the wild type with preheating and CS before and after heat shock (peak A represents the complex; peak B represent the wild type Mj Hsp16.5; peak C represents the intact CS). Inset is the SDS-PAGE analysis of the pool peak A. [Color figure can be viewed in the online issue, which is available at wileyonlinelibrary.com.]

fibril formation of the amyloidogenic peptide dansyl-SSTSAA-W. As ΔNΔLΔC only differs from ΔNΔC in the absence of the β6-strand exchange loop, it is highly possible that the exchange loop covers some of the hydrophobic surface in ΔNΔC. Bis-ANS experiment also showed that ΔNΔLΔC exposed comparable hydrophobic surface as the WT. The N-terminal of WT Mj Hsp16.5 and other sHSPs are hydrophobic. Truncation mutant of the N-terminal of *M. tuberculosis* Hsp16.3 fails to bind bis-ANS[14] and the N-terminal domain of recombinant murine αB-crystallin binds hydrophobic probe bis-ANS.[34] Thus the minimal α-crystallin domain ΔNΔLΔC is actually more efficient to expose hydrophobic sites for binding the two substrates than the WT. This may explain the high chaperone-like activities of the mutant ΔNΔLΔC at non-heat-shock conditions.

The β-strand exchange loop determines the different dimer interface

We also investigated the role of the β-strand exchange loop involved in the formation of the dimer. The two monomers of Mj Hsp16.5 form a stable dimer using the β-strand exchange loop as the swapping domain.[1] Two distinctly different modes of dimerization have evolved across the kingdoms of life. The non-metazoan sHSPs dimerize through reciprocal interaction between β6 and β2 strands; whereas the metazoan sHSPs dimerize through their extended β6 + 7 strands.[13]

We tried to change the dimer interface of Mj Hsp16.5 by disrupting the β-strand exchange loop. Structure alignment showed that the mutant ΔNΔLΔC of Mj Hsp16.5 has a similar β-sandwich fold and similar length of the loop region as the α-crystallin domain from human αB-crystallin (Supporting Information Fig. S2), while the mutant ΔNΔC keeps the original length of the loop region. The mutant ΔNΔC existed as a stable dimer, without concentration dependence. The mutant ΔNΔLΔC, which lacks the β-strand exchange loop present in ΔNΔC, existed as a flexible quaternary structure with a combination of oligomers of different size, and was clearly concentration dependent. Disruption of the domain swapping β-strand [Fig. 1(B)] changed the stable and monodisperse ΔNΔC to the flexible and polydisperse ΔNΔLΔC. Previous X-ray crystallography revealed three distinct alternative registers formed by the paired β6 + 7 strands, termed AP_I , AP_{II}, and AP_{III}.[16] There are differences in the length of β7 in the reported metazoan structure and in how the AP interface forms with regard to registration of hydrogen bonding between the β7 strand.[12,35,36] Whether the variation in the AP interface contributes to the polydispersity of metazoan sHSPs is still under debate.[12] Feil *et al.* used SAXS to study the structure of a truncated form of human αB-crystallin. They found that the dimer interface was flexible with an extended exposed surface area that might contribute to the biological activity and polydispersity of human αB-crystallin.[33] Our result showed that the minimal α-crystallin domain of Mj Hsp16.5 itself (ΔNΔLΔC) is polydisperse and highly active. As the minimal α-crystallin domain of Mj Hsp16.5 is similar to that in the metazoan sHSPs, it is possible that the exposed surface area in metazoan sHSPs may also benefit their chaperone-like activities at non-heat-shock conditions.

Mj Hsp16.5 uses different mechanisms of chaperone-like activities for different substrates

The minimal α-crystallin domain of Mj Hsp16.5 alone was sufficient to exhibit chaperone-like activity to suppress substrate aggregation at non-heat-shock conditions. However, neither of the two mutants can suppress the thermal aggregation of CS. This result is in accord with the fact that the N-31 deleted mutation of Mj Hsp16.5 fails to protect *E. coli* cell extract from thermal aggregation.[6]

To explain the differences in chaperone-like activities for different substrates, we used gel filtration to analyze the properties of chaperone-substrate complex formation. Mj Hsp16.5 shows efficient chaperone-like activity to prevent the thermal aggregation of SCM and *E. coli* cell extract at 80°C, and a tight complex is formed between Mj Hsp16.5 and SCM.[6,9] Other sHSPs, like *M. tuberculosis* Hsp16.3, yeast Hsp26, murine Hsp25, and bovine α-crystallin, can also form complexes with the insulin B chain to suppress its aggregation.[14,37,38] In the present study, we showed that Mj Hsp16.5 did not form a tight complex that could not be separated by gel filtration with the substrates insulin B chain or the amyloidogenic peptide at non-heat-shock conditions. The mutant protein ΔNΔLΔC also could not form tight complex with these substrates, though it showed better chaperone-like activity than the WT. Mj Hsp16.5 formed a complex with the substrate CS to inhibit its thermal aggregation, while the mutant proteins ΔNΔLΔC and ΔNΔC did not.

Our study shows that Mj Hsp16.5 uses two different mechanisms to protect proteins from aggregation. The minimal α-crystallin domain contributes to the chaperone-like activity by transiently interacting with the substrates at non-heat-shock conditions, while the N- and C-terminals and oligomerization were necessary for forming complexes with the substrates to prevent thermal aggregation. This is consistent with reports that the N-terminal domain is essential for complex formation with substrates, when suppressing protein aggregation.[6,14,31,39] To inhibit aggregation of the insulin B chain and fibril formation of the amyloidogenic peptide under non-heat-shock conditions, transient hydrophobic interactions between the substrates and the hydrophobic surface of Mj Hsp16.5 played key role in the inhibition. The sphere of Mj Hsp16.5 24mer is reported to

accumulate and adhere to the already formed hydrophobic fibrils with its hydrophobic surface to slow down the fibrils growth.[8] Under this condition, Mj Hsp16.5 did not dissociate, no subunit exchange occurred, and no tight complex was formed between Mj Hsp16.5 and the substrates. Since most of the hydrophobic region was buried by the subunit interface, the chaperone-like activity was not efficient. The mutant protein ΔNΔLΔC showed better chaperone-like activity due to more hydrophobic exposure than the mutant ΔNΔC. This kind of transient hydrophobic interaction is also reported for the chaperone-like activity of α-crystallin on the inhibition of fibril formation of apoC-II.[40] sHSPs αB-crystallin, Hsp27, Hsp20 bind to α-synuclein to protect its aggregation through a similar weak and transient interaction.[41] As this transient hydrophobic interaction on the surface was not sufficiently tight, and substrates could escape from the small heat shock protein and aggregate at higher temperature, thus the mutants ΔNΔLΔC and ΔNΔC failed to suppress the thermal aggregation of CS. Under heat-shock conditions, especially at temperature relevant for *M. jannaschii*, Mj Hsp16.5 displays structure dynamics, and the 24mers are reported to largely aggregate into unstructured agglomerates and freely and reversibly exchange subunit with surface exposure of hydrophobic patches.[42] A tight complex was formed between Mj Hsp16.5 and the unfolded substrates, when the substrates could not easily escape from the complex to aggregate. This explained the efficient chaperone-like activities of Mj Hsp16.5 under heat-shock conditions. Similar phenomena of temperature-dependent properties of complex formation occur in Pea Hsp18.1 with the substrate CS. CS binding to Hsp18.1 at 38°C is transient and can be reversed at lower temperatures, while at temperature higher than 45°C, Hsp18.1 suppresses the aggregation of CS by irreversible binding, and cooling does not lead to CS reactivation.[43] A recent work also shows αB-crystallin uses different mechanisms of chaperone action. It forms complexes with lactalbumin to prevent its amorphous aggregation, but prevents fibril formation via weak, transient interactions. Complex formation is not the only mechanism used by sHSPs to prevent protein aggregation.[44] The conformational stability of substrate intermediate plays a key role in modulating the mechanism of action and αB-crystallin forms complexes with more destabilized forms of substrates. Stable complexes were formed when the free energy of binding to the chaperone was comparable with the free energy of refolding.[44,45] Our proposed mechanism was consistent with these experiment results.

CONCLUSIONS

In conclusion, by deleting the N- and C-terminals and the β-strand exchange loop, we find that the minimal α-crystallin domain of Mj Hsp16.5 forms a polydisperse quaternary structure and is functional at non-heat-shock conditions. We demonstrate experimentally that the β-strand exchange loop covers the hydrophobic surface for substrates binding and determines the dimer interface of Mj Hsp16.5. We propose that Mj Hsp16.5 uses different mechanisms for its chaperone-like activities to protect different substrates. It protects substrates from aggregation by transient hydrophobic interactions under non-heat-shock conditions, while it suppresses the thermal aggregation by forming tight complexes with the substrates.

REFERENCES

1. Kim KK, Kim R, Kim SH. Crystal structure of a small heat-shock protein. Nature 1998;394(6693):595–599.
2. Cao A, Wang Z, Wei P, Xu F, Cao J, Lai L. Preheating induced homogeneity of the small heat shock protein from *Methanococcus jannaschii*. Biochim Biophys Acta 2008;1784(3):489–495.
3. Horwitz J. The function of alpha-crystallin in vision. Sem Cell Dev Biol 2000;11(1):53–60.
4. Van Montfort RL, Basha E, Friedrich KL, Slingsby C, Vierling E. Crystal structure and assembly of a eukaryotic small heat shock protein. Nat Struct Biol 2001;8(12):1025–1030.
5. Sun Y, MacRae TH. The small heat shock proteins and their role in human disease. FEBS J 2005;272(11):2613–2627.
6. Kim R, Lai L, Lee HH, Cheong GW, Kim KK, Wu Z, Yokota H, Marqusee S, Kim SH. On the mechanism of chaperone activity of the small heat-shock protein of *Methanococcus jannaschii*. Proc Natl Acad Sci USA 2003;100(14):8151–8155.
7. Bova MP, Huang Q, Ding L, Horwitz J. Subunit exchange, conformational stability, and chaperone-like function of the small heat shock protein 16.5 from *Methanococcus jannaschii*. J Biol Chem 2002;277(41):38468–38475.
8. Xi D, Dong X, Deng W, Lai L. Dynamic behavior of small heat shock protein inhibition on amyloid fibrillization of a small peptide (SSTSAA) from RNase A. Biochem Biophys Res Commun 2011; 416(1-2):130–134.
9. Kim R, Kim KK, Yokota H, Kim SH. Small heat shock protein of *Methanococcus jannaschii*, a hyperthermophile. Proc Natl Acad Sci USA 1998;95(16):9129–9133.
10. Bagneris C, Bateman OA, Naylor CE, Cronin N, Boelens WC, Keep NH, Slingsby C. Crystal Structures of alpha-crystallin domain dimers of alpha B-crystallin and Hsp20. J Mol Biol 2009;392(5): 1242–1252.
11. Maitre M, Weidmann S, Rieu A, Fenel D, Schoehn G, Ebel C, Coves J, Guzzo J. The oligomer plasticity of the small heat-shock protein Lo18 from Oenococcus oeni influences its role in both membrane stabilization and protein protection. Biochem J 2012;444(1):97–104.
12. Basha E, O'Neill H, Vierling E. Small heat shock proteins and alpha-crystallins: dynamic proteins with flexible functions. Trends Biochem Sci 2012;37(3):106–117.
13. Hilton GR, Lioe H, Stengel F, Baldwin AJ, Benesch JL. Small heat-shock proteins: paramedics of the cell. Top Curr Chem 2013;328: 69–98.
14. Fu X, Zhang H, Zhang X, Cao Y, Jiao W, Liu C, Song Y, Abulimiti A, Chang Z. A dual role for the N-terminal region of *Mycobacterium tuberculosis* Hsp16.3 in self-oligomerization and binding denaturing substrate proteins. J Biol Chem 2005;280(8):6337–6348.
15. Basha E, Friedrich KL, Vierling E. The N-terminal arm of small heat shock proteins is important for both chaperone activity and substrate specificity. J Biol Chem 2006;281(52):39943–39952.
16. Laganowsky A, Benesch JL, Landau M, Ding L, Sawaya MR, Cascio D, Huang Q, Robinson CV, Horwitz J, Eisenberg D. Crystal

structures of truncated alphaA and alphaB crystallins reveal structural mechanisms of polydispersity important for eye lens function. Protein Sci 2010;19(5):1031–1043.
17. Jehle S, Rajagopal P, Bardiaux B, Markovic S, Kuhne R, Stout JR, Higman VA, Klevit RE, Van Rossum BJ, Oschkinat H. Solid-state NMR and SAXS studies provide a structural basis for the activation of alphaB-crystallin oligomers. Nat Struct Mol Biol 2010;17(9): 1037–1042.
18. Kasakov AS, Bukach OV, Seit-Nebi AS, Marston SB, Gusev NB. Effect of mutations in the β5–β7 loop on the structure and properties of human small heat shock protein HSP22 (HspB8, H11). FEBS J 2007;274(21):5628–5642.
19. Mymrikov EV, Seit-Nebi AS, Gusev NB. Large potentials of small heat shock proteins. Physiol Rev 2011;91(4):1123–1159.
20. Breitsprecher D, Kiesewetter AK, Linkner J, Urbanke C, Resch GP, Small JV, Faix J. Clustering of VASP actively drives processive, WH2 domain-mediated actin filament elongation. EMBO J 2008;27(22): 2943–2954.
21. Deng W, Cao A, Lai L. Detecting the inter-peptide arrangement and maturation process of transthyretin (105–115) amyloid fibril using a FRET pair with short Forster distance. Biochem Biophys Res Commun 2007;362(3):689–694.
22. Sudhakar K, Fay PJ. Exposed hydrophobic sites in factor VIII and isolated subunits. J Biol Chem 1996;271(38):23015–23021.
23. Schrodinger, LLC. The PyMOL Molecular Graphics System, Version 1.3r1; 2010.
24. Berendsen HJC, van der Spoel D, van Drunen R. GROMACS: a message-passing parallel molecular dynamics implementation. Comput Phys Commun 1995;91(1-3):43–56.
25. Sugino C, Hirose M, Tohda H, Yoshinari Y, Abe T, Giga-Hama Y, Iizuka R, Shimizu M, Kidokoro S, Ishii N, Yohda M. Characterization of a sHsp of Schizosaccharomyces pombe, SpHsp15.8, and the implication of its functional mechanism by comparison with another sHsp, SpHsp16.0. Proteins 2009;74(1):6–17.
26. Deng W, Cao A, Lai L. Distinguishing the cross-beta spine arrangements in amyloid fibrils using FRET analysis. Protein Sci 2008; 17(6):1102–1105.
27. Augusteyn RC. Alpha-crystallin: a review of its structure and function. Clin Exp Optom 2004;87(6):356–366.
28. Chen J, Feige MJ, Franzmann TM, Bepperling A, Buchner J. Regions outside the alpha-crystallin domain of the small heat shock protein Hsp26 are required for its dimerization. J Mol Biol 2010;398(1): 122–131.
29. Giese KC, Basha E, Catague BY, Vierling E. Evidence for an essential function of the N terminus of a small heat shock protein in vivo, independent of in vitro chaperone activity. Proc Natl Acad Sci USA 2005;102(52):18896–18901.
30. Studer S, Obrist M, Lentze N, Narberhaus F. A critical motif for oligomerization and chaperone activity of bacterial alpha-heat shock proteins. Eur J Biochem 2002;269(14):3578–3586.
31. Stromer T, Fischer E, Richter K, Haslbeck M, Buchner J. Analysis of the regulation of the molecular chaperone Hsp26 by temperature-induced dissociation: the N-terminal domail is important for oligomer assembly and the binding of unfolding proteins. J Biol Chem 2004;279(12):11222–11228.
32. Leroux MR, Melki R, Gordon B, Batelier G, Candido EP. Structure-function studies on small heat shock protein oligomeric assembly and interaction with unfolded polypeptides. J Biol Chem 1997; 272(39):24646–24656.
33. Feil IK, Malfois M, Hendle J, Van Der Zandt H, Svergun DI. A novel quaternary structure of the dimeric alpha-crystallin domain with chaperone-like activity. J Biol Chem 2001;276(15):12024–12029.
34. Smulders RH, De Jong WW. The hydrophobic probe 4,4′-bis(1-anilino-8-naphthalene sulfonic acid) is specifically photoincorporated into the N-terminal domain of alpha B-crystallin. FEBS Lett 1997; 409(1):101–104.
35. Baldwin AJ, Lioe H, Robinson CV, Kay LE, Benesch JL. AlphaB-crystallin polydispersity is a consequence of unbiased quaternary dynamics. J Mol Biol 2011;413(2):297–309.
36. Jehle S, Van Rossum B, Stout JR, Noguchi SM, Falber K, Rehbein K, Oschkinat H, Klevit RE, Rajagopal P. AlphaB-crystallin: a hybrid solid-state/solution-state NMR investigation reveals structural aspects of the heterogeneous oligomer. J Mol Biol 2009;385(5): 1481–1497.
37. Stromer T, Ehrnsperger M, Gaestel M, Buchner J. Analysis of the interaction of small heat shock proteins with unfolding proteins. J Biol Chem 2003;278(20):18015–18021.
38. Farahbakhsh ZT, Huang QL, Ding LL, Altenbach C, Steinhoff HJ, Horwitz J, Hubbell WL. Interaction of alpha-crystallin with spin-labeled peptides. Biochemistry 1995;34(2):509–516.
39. Haslbeck M, Ignatiou A, Saibil H, Helmich S, Frenzl E, Stromer T, Buchner J. A domain in the N-terminal part of Hsp26 is essential for chaperone function and oligomerization. J Mol Biol 2004; 343(2):445–455.
40. Hatters DM, Lindner RA, Carver JA, Howlett GJ. The molecular chaperone, alpha-crystallin, inhibits amyloid formation by apolipoprotein C-II. J Biol Chem 2001;276(36):33755–33761.
41. Bruinsma IB, Bruggink KA, Kinast K, Versleijen AA, Segers-Nolten IM, Subramaniam V, Kuiperij HB, Boelens W, de Waal RM, Verbeek MM. Inhibition of alpha-synuclein aggregation by small heat shock proteins. Proteins 2011;79(10):2956–2967.
42. Haslbeck M, Kastenmuller A, Buchner J, Weinkauf S, Braun N. Structural dynamics of archaeal small heat shock proteins. J Mol Biol 2008;378(2):362–374.
43. Lee GJ, Roseman AM, Saibil HR, Vierling E. A small heat shock protein stably binds heat-denatured model substrates and can maintain a substrate in a folding-competent state. EMBO J 1997;16(3): 659–671.
44. Kulig M, Ecroyd H. The small heat shock protein alphaB crystallin uses different mechanisms of chaperone action to prevent the amorphous versus fibrillar aggregation of alpha-lactalbumin. Biochem J 2012;448(3):343–352.
45. Koteiche HA, McHaourab HS. Mechanism of chaperone function in small heat-shock proteins. Phosphorylation-induced activation of two-mode binding in alphaB-crystallin. J Biol Chem 2003;278(12): 10361–10367.